Bifurcation Analysis for a Modified Jeffcott Rotor with Bearing Clearances

Y. B. KIM and S. T. NOAH

Mechanical Engineering Department, Texas A&M University, College Station, TX 77843-3123, U.S.A.

Abstract. A HB (Harmonic Balance)/AFT (Alternating Frequency/Time) technique is developed to obtain synchronous and subsynchronous whirling motions of a horizontal Jeffcott rotor with bearing clearances. The method utilizes an explicit Jacobian form for the iterative process which guarantees convergence at all parameter values. The method is shown to constitute a robust and accurate numerical scheme for the analysis of two dimensional nonlinear rotor problems. The stability analysis of the steady-state motions is obtained using perturbed equations about the periodic motions. The Floquet multipliers of the associated Monodromy matrix are determined using a new discrete HB/AFT method. Flip bifurcation boundaries were obtained which facilitated detection of possible rotor chaotic (irregular) motion as parameters of the system are changed. Quasi-periodic motion is also shown to occur as a result of a secondary Hopf bifurcation due to increase of the destabilizing cross-coupling stiffness coefficients in the rotor model.

Key words: Nonlinear, rotor, clearance, chaos.

1. Introduction

Many rotor dynamic systems exhibit nonlinear behavior due to bearing clearances, squeeze film dampers, seals and fluid dynamics effects. Nonlinear rotor systems involving bearing clearances were studied by several investigators. Bently [1] used a simple horizontal rotor model with a bearing clearance to explain the occurrence of subharmonics in his experimental results. Childs [2] used a perturbation technique to study the occurrence of subharmonics, assuming small nonlinearity for the bearing clearance. Saito [3] utilized a harmonic balance method (HBM) along with a fast Fourier transform (FFT) procedure, which was originally used by Yamauchi [4], to explain some nonlinear characteristics in a Jeffcott rotor on nonlinear supports. Choi and Noah [5] also used the HBM with FFT to show the occurrence of super and subharmonics in a rotor in presence of a bearing clearance. In [3] and [5], numerical differentiation was used within each iterative cycle. This did frequently lead to difficulties in getting consistent convergence in all parameter ranges. A numerical approach based on a collocation technique was adopted by Nataraj and Nelson [6] and used to obtain periodic whirling motions in nonlinear rotor systems. In their approach, the calculation of eigenvalues and eigenvectors is required to obtain steady-state rotor whirling motions. This could have the disadvantage of making the numerical process more elaborate and lengthy. Nevertheless, the method appears to be versatile and effective. Ehrich [7] used numerical integration to show the occurrence of higher subharmonics (up to 9th order) in a high speed rotor system with a bearing clearance.

Simulations revealing aperiodic whirling motion were reported by Childs [8]. Day [9] proposed an interpretation involving a 'nonlinear natural frequency' to explain the occurrence of aperiodic motion obtained using the multiple scales method.

Nonlinear Dynamics **1**: 221–241, 1990

Few analysts have addressed the stability of periodic or subharmonic responses of nonlinear rotor systems despite its considerable significance in the development and analysis of modern high performance rotor systems. Most of the stability or bifurcation analyses were concentrated on one dimensional problems where motion patterns are assumed apriori (Shaw and Holmes [10] and Natsiavas [11]). These approaches could be proved unfeasible to extend to two dimensional nonlinear rotor problems in which, say, whirling motion involving intermittent contact with a bearing clearance would occur.

This paper addresses the response and stability of a modified Jeffcott rotor system with a discontinuous nonlinearity (bearing clearances). The paper consists of two parts. First, a modified HBM is developed which combines an exact Jacobian matrix and a Galerkin procedure to formulate a robust iterative procedure for determining the periodic solutions. Second, a new approach for the stability analysis of the periodic whirling is developed and applied to conduct bifurcation analysis of the rotor system and search for possible chaotic responses.

Equations of Motion

The equations of motion for a horizontal Jeffcott rotor with bearing clearances (refer to Figure 1) can be written as

$$mX'' + cX' + k_s X + Q_s Y + \Phi k_b X\left(1 - \frac{\delta}{\sqrt{X^2 + Y^2}}\right) - \mu \Phi k_b Y\left(1 - \frac{\delta}{\sqrt{X^2 + Y^2}}\right) = me\omega^2 \cos \omega t\,, \tag{1a}$$

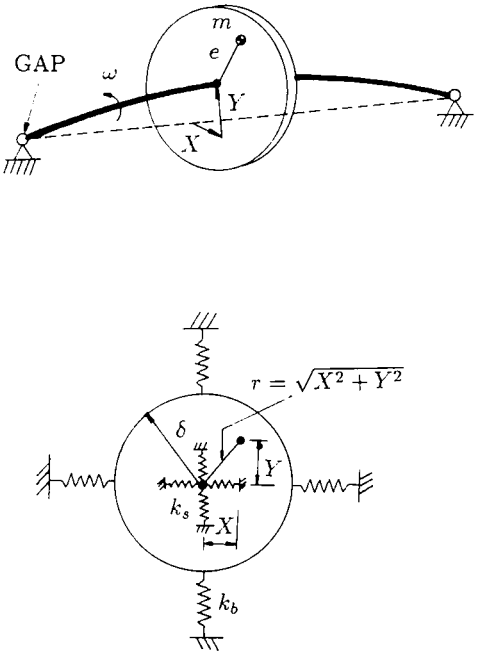

Fig. 1. Jeffcott rotor model with bearing clearances (refer to [7]).

$$mY'' + cY' + k_s Y - Q_s X + \Phi k_b Y\left(1 - \frac{\delta}{\sqrt{X^2 + Y^2}}\right) + \mu \Phi k_b X\left(1 - \frac{\delta}{\sqrt{X^2 + Y^2}}\right)$$
$$= me\omega^2 \sin \omega t - mg \,, \tag{1b}$$

where k_s is the shaft stiffness, Q_s is the cross coupling stiffness, c is the system damping, μ is the friction coefficient, δ is the radial clearance of the bearing. A prime represents a derivative with respect to time t and

$$\Phi = \begin{cases} 1, & \sqrt{X^2 + Y^2} > \delta \,, \\ 0, & \sqrt{X^2 + Y^2} \leqslant \delta \,. \end{cases}$$

To study the effect of the parameters on the behavior of the system, the following nondimensional groups are introduced: $\omega_n = \sqrt{K/m}$, $K = 4k_s k_b/(\sqrt{k_s} + \sqrt{k_b})^2$, $x = X/e$, $y = Y/e$, $\Omega = \omega/\omega_n$, $\zeta = c/2m\omega_n$, $\gamma = Q_s/K$, $\alpha = k_b/k_s$, $\delta^* = \delta/e$, $\phi = g/\omega_n^2 e$, $r^* = \sqrt{x^2 + y^2}$, and $\nu\theta = \omega t$. Here ν represents the subharmonic ratios. ($\nu = 1$ for harmonic and superharmonic cases, and $\nu = n$ for an nth subharmonic case.) Equation (1) can now be written as

$$\ddot{x} + \frac{2\zeta\nu}{\Omega}\dot{x} + \frac{\nu^2}{\Omega^2}\frac{(1 + \sqrt{\alpha})^2}{4\alpha}x + \gamma\frac{\nu^2}{\Omega^2}y + T(\theta) - \mu F(\theta) = \nu^2 \cos \nu\theta \,, \tag{2a}$$

$$\ddot{y} + \frac{2\zeta\nu}{\Omega}\dot{y} + \frac{\nu^2}{\Omega^2}\frac{(1 + \sqrt{\alpha})^2}{4\alpha}y - \gamma\frac{\nu^2}{\Omega^2}x + F(\theta) + \mu T(\theta) = \nu^2 \sin \nu\theta - \phi\frac{\nu^2}{\Omega^2} \,, \tag{2b}$$

where a dot represents a derivative with respect to the nondimensional time θ and Φ is unity if r^* is greater than δ^*, otherwise it is zero. $T(\theta)$ and $F(\theta)$ are given by the following expressions.

$$T(\theta) = \Phi\frac{\nu^2}{\Omega^2}\frac{(1 + \sqrt{\alpha})^2}{4}x\left(1 - \frac{\delta^*}{\sqrt{x^2 + y^2}}\right),$$

$$F(\theta) = \Phi\frac{\nu^2}{\Omega^2}\frac{(1 + \sqrt{\alpha})^2}{4}y\left(1 - \frac{\delta^*}{\sqrt{x^2 + y^2}}\right),$$

where

$$\Phi = \begin{cases} 1, & \sqrt{x^2 + y^2} > \delta^* \,, \\ 0, & \sqrt{x^2 + y^2} \leqslant \delta^* \,. \end{cases}$$

After reaching the steady-state, and assuming periodic whirl, the solution forms of x and y can be represented as

$$x(\theta) = a_{x0} + \sum_{n=1}^{N} (a_{xn} \cos n\theta - b_{xn} \sin n\theta) \,, \tag{3a}$$

$$y(\theta) = a_{y0} + \sum_{n=1}^{N} (a_{yn} \cos n\theta - b_{yn} \sin n\theta) \,. \tag{3b}$$

The nonlinear restoring forces of $T(\theta)$ and $F(\theta)$ are also expressed as

$$T(\theta) = c_{x0} + \sum_{n=1}^{N} (c_{xn} \cos n\theta - d_{xn} \sin n\theta) , \tag{4a}$$

$$F(\theta) = c_{y0} + \sum_{n=1}^{N} (c_{yn} \cos n\theta - d_{xn} \sin n\theta) . \tag{4b}$$

In equations (3) and (4), N represents the maximum number of harmonic terms considered. Inserting equations (3) and (4) into (2), and equating the coefficients of $\sin(n\theta)$ and $\cos(n\theta)$ on both sides of the equations, one arrives at the following implicitly nonlinear algebraic equations

for the constant series terms

$$g(1) = \frac{\nu^2}{\Omega^2} \frac{(1+\sqrt{\alpha})^2}{4\alpha} a_{x0} + \gamma \frac{\nu^2}{\Omega^2} a_{y0} + c_{x0} - \mu c_{y0} = 0 \tag{5}$$

$$g(2) = \frac{\nu^2}{\Omega^2} \frac{(1+\sqrt{\alpha})^2}{4\alpha} a_{y0} - \gamma \frac{\nu^2}{\Omega^2} a_{x0} + c_{y0} + \mu c_{x0} + \phi \frac{\nu^2}{\Omega^2} = 0 , \tag{6}$$

for the trigonometric series terms

$$g(4n-1) = -n^2 a_{xn} - \frac{2\zeta\nu n}{\Omega} b_{xn} + \frac{\nu^2}{\Omega^2} \frac{(1+\sqrt{\alpha})^2}{4\alpha} a_{xn} + \gamma \frac{\nu^2}{\Omega^2} a_{yn} + c_{xn} - \mu c_{yn} - \Psi(n)\nu^2 = 0 \tag{7}$$

$$g(4n) = n^2 b_{xn} - \frac{2\zeta\nu n}{\Omega} a_{xn} - \frac{\nu^2}{\Omega^2} \frac{(1+\sqrt{\alpha})^2}{4\alpha} b_{xn} - \gamma \frac{\nu^2}{\Omega^2} b_{yn} - d_{xn} + \mu d_{yn} = 0 \tag{8}$$

$$g(4n+1) = -n^2 a_{yn} - \frac{2\zeta\nu n}{\Omega} b_{yn} + \frac{\nu^2}{\Omega^2} \frac{(1+\sqrt{\alpha})^2}{4\alpha} a_{yn} - \gamma \frac{\nu^2}{\Omega^2} a_{xn} + c_{yn} + \mu c_{xn} = 0 \tag{9}$$

$$g(4n+2) = n^2 b_{yn} - \frac{2\zeta\nu n}{\Omega} a_{yn} + \frac{\nu^2}{\Omega^2} \frac{(1+\sqrt{\alpha})^2}{4\alpha} b_{yn} + \gamma \frac{\nu^2}{\Omega^2} b_{xn} - d_{yn} - \mu d_{xn} - \Psi(n)\nu^2 = 0 . \tag{10}$$

In the above equations, $\Psi(n)$ is unity if $n = \nu$, otherwise $\Psi(n)$ has zero value, and $n = 1, 2, \ldots, N$.

Let the unknown vector $\mathbf{P}$ of the displacement coefficients be defined as

$$\mathbf{P} = [a_{x0}, a_{y0}, a_{x1}, b_{x1}, a_{y1}, b_{y1}, \ldots, a_{yN}, b_{yN}]^T \tag{11a}$$

and the unknown restoring vector $\mathbf{Q}$ of the force coefficients be expressed as

$$\mathbf{Q} = [c_{x0}, c_{y0}, c_{x1}, d_{x1}, c_{y1}, d_{y1}, \ldots, c_{yN}, d_{yN}]^T , \tag{11b}$$

where T stands for the transpose. The Newton–Raphson method can be used for this two-dimensional rotor problem to solve for the unknown vectors $\mathbf{P}$ and $\mathbf{Q}$. Alternatively, using equations (5)–(10) another iterative scheme such as the Broyden method [12] can be used to obtain the steady-state solutions in which calculation of the Jacobian matrix would be avoided. Broyden method converges more slowly (usually it requires more iteration steps) but possesses

larger radii of convergence for initial guesses. In this study, Newton–Raphson method is used, since an explicit form of the Jacobian was made available.

Newton–Raphson Approach

Equations (5)–(10) are nonlinear algebraic equations whose solutions yield **P**. A system of linear equations for the correction increments $\Delta\mathbf{P}$ of the unknown coefficients can be written as

$$[J]\Delta\mathbf{P} + \mathbf{G} = 0\,, \tag{12}$$

where $[J] = [\partial\mathbf{G}/\partial\mathbf{P}]$ is the associated Jacobian (matrix of first order derivatives) whose elements are listed in Appendix A, and **G** is a $(4N + 2)$ column vector whose element $g(1), \ldots, g(4n + 2)$ are given by equations (5)–(10).

Using an AFT method [13], the nonlinear force vector **Q** can readily be obtained from the unknown vector **P**. An IDFT is first employed to obtain discrete displacements of x and y from **P** which in turn are used to calculate corresponding discrete values of the nonlinear forces. A DFT procedure is then used to calculate the **Q** vector from these discrete nonlinear forces. As **Q** is a function of **P**, the Jacobian matrix, $[J]$, has the components of $\partial\mathbf{Q}/\partial\mathbf{P}$ which are expressed as

$$\frac{\partial c_{xn}}{\partial a_{xl}} = \frac{1}{M}\sum_{r=0}^{M-1} A_r \cos\frac{2\pi lr}{M}\cos\frac{2\pi nr}{M}\,, \qquad \frac{\partial c_{xn}}{\partial b_{xl}} = -\frac{1}{M}\sum_{r=0}^{M-1} A_r \sin\frac{2\pi lr}{M}\cos\frac{2\pi nr}{M}\,,$$

$$\frac{\partial c_{xn}}{\partial a_{yl}} = -\frac{1}{M}\sum_{r=0}^{M-1} B_r \cos\frac{2\pi lr}{M}\cos\frac{2\pi nr}{M}\,, \qquad \frac{\partial c_{xn}}{\partial b_{yl}} = \frac{1}{M}\sum_{r=0}^{M-1} B_r \sin\frac{2\pi lr}{M}\cos\frac{2\pi nr}{M}\,,$$

$$\frac{\partial d_{xn}}{\partial a_{xl}} = -\frac{1}{M}\sum_{r=0}^{M-1} A_r \cos\frac{2\pi lr}{M}\sin\frac{2\pi nr}{M}\,, \qquad \frac{\partial d_{xn}}{\partial b_{xl}} = \frac{1}{M}\sum_{r=0}^{M-1} A_r \sin\frac{2\pi lr}{M}\sin\frac{2\pi nr}{M}\,,$$

$$\frac{\partial d_{xn}}{\partial a_{yl}} = \frac{1}{M}\sum_{r=0}^{M-1} B_r \cos\frac{2\pi lr}{M}\sin\frac{2\pi nr}{M}\,, \qquad \frac{\partial d_{xn}}{\partial b_{yl}} = -\frac{1}{M}\sum_{r=0}^{M-1} B_r \sin\frac{2\pi lr}{M}\sin\frac{2\pi nr}{M}\,,$$

$$\frac{\partial c_{yn}}{\partial a_{xl}} = -\frac{1}{M}\sum_{r=0}^{M-1} C_r \cos\frac{2\pi lr}{M}\cos\frac{2\pi nr}{M}\,, \qquad \frac{\partial c_{yn}}{\partial b_{xl}} = \frac{1}{M}\sum_{r=0}^{M-1} C_r \sin\frac{2\pi lr}{M}\cos\frac{2\pi nr}{M}\,,$$

$$\frac{\partial c_{yn}}{\partial a_{yl}} = \frac{1}{M}\sum_{r=0}^{M-1} D_r \cos\frac{2\pi lr}{M}\cos\frac{2\pi nr}{M}\,, \qquad \frac{\partial c_{yn}}{\partial b_{yl}} = -\frac{1}{M}\sum_{r=0}^{M-1} D_r \sin\frac{2\pi lr}{M}\cos\frac{2\pi nr}{M}\,,$$

$$\frac{\partial d_{yn}}{\partial a_{xl}} = \frac{1}{M}\sum_{r=0}^{M-1} C_r \cos\frac{2\pi lr}{M}\sin\frac{2\pi nr}{M}\,, \qquad \frac{\partial d_{yn}}{\partial b_{xl}} = -\frac{1}{M}\sum_{r=0}^{M-1} C_r \sin\frac{2\pi lr}{M}\sin\frac{2\pi nr}{M}\,,$$

$$\frac{\partial d_{yn}}{\partial a_{yl}} = -\frac{1}{M}\sum_{r=0}^{M-1} D_r \cos\frac{2\pi lr}{M}\sin\frac{2\pi nr}{M}\,, \qquad \frac{\partial d_{yn}}{\partial b_{yl}} = \frac{1}{M}\sum_{r=0}^{M-1} D_r \sin\frac{2\pi lr}{M}\sin\frac{2\pi nr}{M}\,; \tag{13}$$

$n, l = 1, 2, \ldots, N$, where

$$A_r = \left[\frac{\nu^2}{\Omega^2}\,\frac{(1+\sqrt{\alpha})^2}{4\alpha} - \frac{\nu^2}{\Omega^2}\,\frac{(1+\sqrt{\alpha})^2}{4\alpha}\,\delta^*(x^2+y^2)^{(-3/2)}y^2\right]_r\,,$$

$$B_r = \left[-\frac{\nu^2}{\Omega^2} \frac{(1+\sqrt{\alpha})^2}{4\alpha} \delta^*(x^2+y^2)^{(-3/2)}xy \right]_r ,$$

$$C_r = \left[-\frac{\nu^2}{\Omega^2} \frac{(1+\sqrt{\alpha})^2}{4\alpha} \delta^*(x^2+y^2)^{(-3/2)}xy \right]_r ,$$

$$D_r = \left[\frac{\nu^2}{\Omega^2} \frac{(1+\sqrt{\alpha})^2}{4\alpha} - \frac{\nu^2}{\Omega^2} \frac{(1+\sqrt{\alpha})^2}{4\alpha} \delta^*(x^2+y^2)^{(-3/2)}x^2 \right]_r$$

and M is the total number of discrete data points in the time domain. More details about the calculation procedure can be found in Appendix B.

The procedure of using the Newton–Raphson method to determine a periodic solution can be summed up as follows:

(1) Assume an initial value, $\mathbf{P}^{(0)}$, of the coefficient vector $\mathbf{P}$.
(2) At a given iteration step, evaluate $\mathbf{Q}^{(k)}$ from $\mathbf{P}^{(k)}$ by using the AFT method.
(3) Calculate $[J]$ and $\mathbf{G}$.
(4) Solve equation (12) to determine the correction vector $\Delta\mathbf{P}$.
(5) End iteration if $(\Delta\mathbf{P}^{(k)} - \Delta\mathbf{P}^{(k-1)})$ is within a specified error bound, otherwise set $\mathbf{P}^{(k+1)} = \mathbf{P}^{(k)} + \Delta\mathbf{P}^{(k)}$ and return to step (2). For obtaining possible multiple solutions, different initial guesses could be selected at step (1).

Stability Analysis

One of the advantages of the HBM with an AFT procedure is that it readily provides stability criteria as well as information concerning bifurcation behavior. In rotor systems, stability and bifurcation analysis of a given periodic solution can offer valuable design inputs to avoid sudden change of behavior, irregular (chaotic) motion, and dangerous subsynchronous or supersynchronous vibrations. To investigate the stability behavior of a 2π-periodic solution, eigenvalues of the associated monodromy matrix are utilized [14].

For the stability analysis, the second order nonlinear ordinary differential equations of the present two dimensional problem are perturbed about the determined periodic solution under consideration. This leads to the following perturbed equations

$$\Delta\ddot{x} + \frac{2\zeta\nu}{\Omega}\Delta\dot{x} + \frac{\nu^2}{\Omega^2}\frac{(1+\sqrt{\alpha})^2}{4\alpha}\Delta x + \gamma\frac{\nu^2}{\Omega^2}\Delta y + A\Delta x - B\Delta y + \mu C\Delta x - \mu D\Delta y = 0 , \qquad (14a)$$

$$\Delta\ddot{y} + \frac{2\zeta\nu}{\Omega}\Delta\dot{y} + \frac{\nu^2}{\Omega^2}\frac{(1+\sqrt{\alpha})^2}{4\alpha}\Delta y - \gamma\frac{\nu^2}{\Omega^2}\Delta x - C\Delta x + D\Delta y + \mu A\Delta x - \mu B\Delta y = 0 , \qquad (14b)$$

where A, B, C, and D have the same expressions as given previously. Equations (14) are ordinary differential equations with periodic coefficients, since A, B, C, and D are 2π-*periodic*. Equations (14a) and (14b) are cast in first order form, or

$$\dot{\mathbf{p}} = [u(\theta)]\mathbf{p} , \qquad (15)$$

where $\mathbf{p} = [\Delta x, \Delta y, \Delta\dot{x}, \Delta\dot{y}]^T$, and $[u(\theta)]$ is the matrix defined as

$$[u(\theta)] = \begin{pmatrix} 0 & 0 & 1 & 0 \\ 0 & 0 & 0 & 1 \\ -q_1(\theta) & -q_2(\theta) & \dfrac{-2\zeta\nu}{\Omega} & 0 \\ -q_3(\theta) & -q_4(\theta) & 0 & \dfrac{-2\zeta\nu}{\Omega} \end{pmatrix} \tag{16}$$

and

$$q_1(\theta) = \frac{\nu^2}{\Omega^2}\,\frac{(1+\sqrt{\alpha})^2}{4\alpha} + A + \mu C$$

$$q_2(\theta) = \gamma\,\frac{\nu^2}{\Omega^2} - B - \mu D$$

$$q_3(\theta) = -\gamma\,\frac{\nu^2}{\Omega^2} - C + \mu A$$

$$q_4(\theta) = \frac{\nu^2}{\Omega^2}\,\frac{(1+\sqrt{\alpha})^2}{4\alpha} + D - \mu B\,.$$

Let the monodromy matrix be denoted by $[R]$, and satisfy the following ordinary differential matrix equation

$$[\dot{R}] = [u(\theta)][R]\,; \qquad [R(0)] = [I]\,, \tag{17}$$

where $[I]$ is the identity matrix. Without loss of generality, the initial conditions are assumed as the identity matrix. The monodromy matrix can be calculated by integrating equation (17) numerically from time 0 to one period, 2π. The eigenvalues of the monodromy matrix are the Floquet multipliers which are used to determine the stability of the 2π-periodic solutions as follows, [15],

1. If all the multipliers are located within the unit circle, the system is stable.
2. If one of the multipliers leave the unit circle through -1, this indicates period multiplying bifurcations.
3. If one of the multipliers leaves the unit circle through $+1$, this could indicate bifurcations, possibly including a saddle node.
4. If a pair of complex conjugate multipliers is leaving the unit circle, a Hopf, or a secondary Hopf bifurcation could occur.

Numerical Results and Discussion

Among the seven nondimensional parameters (Ω, ζ, γ, α, δ^*, ϕ, μ), the magnitudes of $\delta^* = 30$ and $\phi = 30 \times$ stiffness ($=(1+\sqrt{\alpha})^2/4\alpha$) were selected so as to satisfy the condition that the rotor center offset equals to the clearance (normal tightening condition [2]). The other five parameters were varied. The normal tightening condition not only reduces the number of parameter variation effects to be studied, but also fulfills the same whirling motions which were reported experimentally. This condition is necessary for intermittent rotor/bearing contacts to occur, constituting the

main nonlinearity of the system in the y direction. Figures 2, 3, and 4 display the same whirling shapes as obtained by Ehrich [7] within the same parameter ranges, as will be discussed below.

Periodic Response

The accuracy of the HBM/AFT utilizing a Newton–Raphson algorithm (hereafter the HBM/AFT is used to indicate the HBM/AFT with Newton–Raphson for convenience) is compared with numerical integration (4th order Runge–Kutta) as shown in Figures 2, 3 and 4. Figure 2 shows a period-1 whirling orbit at $\Omega = 1.1$. The figure shows very good accuracy of the HBM/AFT. Figures 3, 4 show a period-2 (2nd subharmonic) and a period-3 (3rd subharmonic) whirling response at $\Omega = 2.2$ and $\Omega = 3.2$, respectively. Again, these figures show the HBM/AFT method to be very accurate. Note that small discrepancies in higher subharmonic orbits are due to truncation of higher harmonic terms in the assumed steady state solutions. For the results presented herein, up to 4 harmonic terms were considered which combined good accuracy with high computational efficiency. The other iterative scheme of Broyden also converges to the same orbits as shown in Figures 2, 3, and 4 with comparable accuracy. The major difference between these two methods is that the HBM/AFT converges much faster than the Broyden but requires more narrow domain of

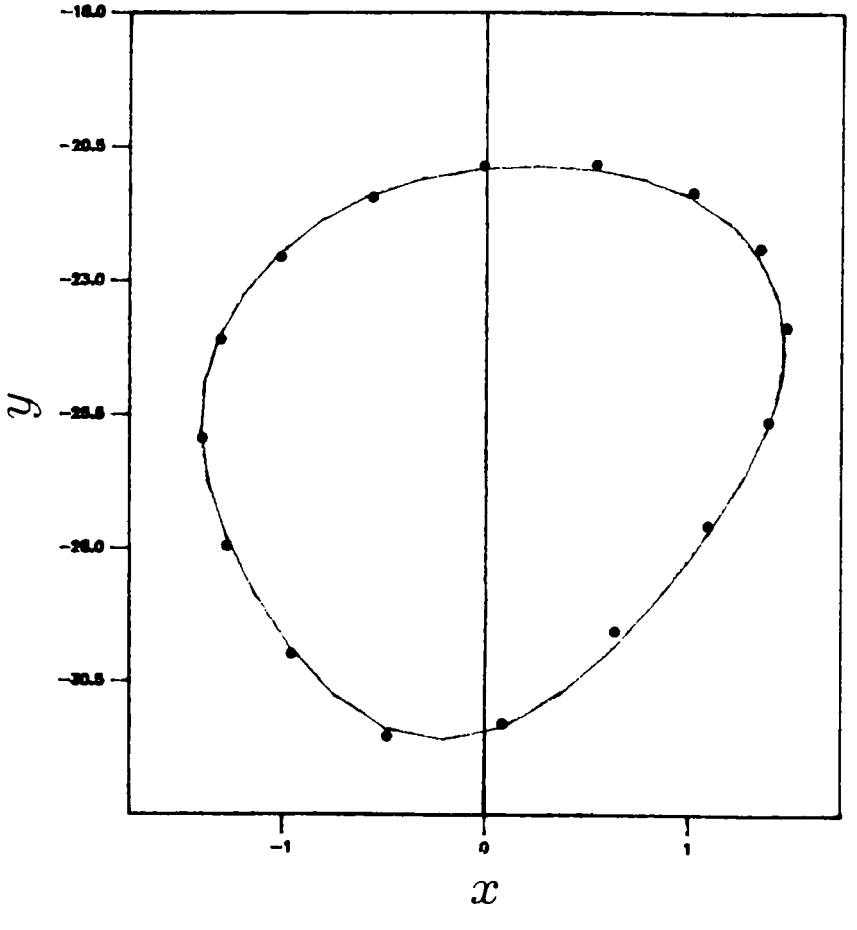

Fig. 2. Orbit-1 whirling motion ($\alpha = 25$, $\zeta = 0.02$, $\Omega = 1.1$, $\gamma = 0$, $\mu = 0$) — HBM; . . . Runge–Kutta.

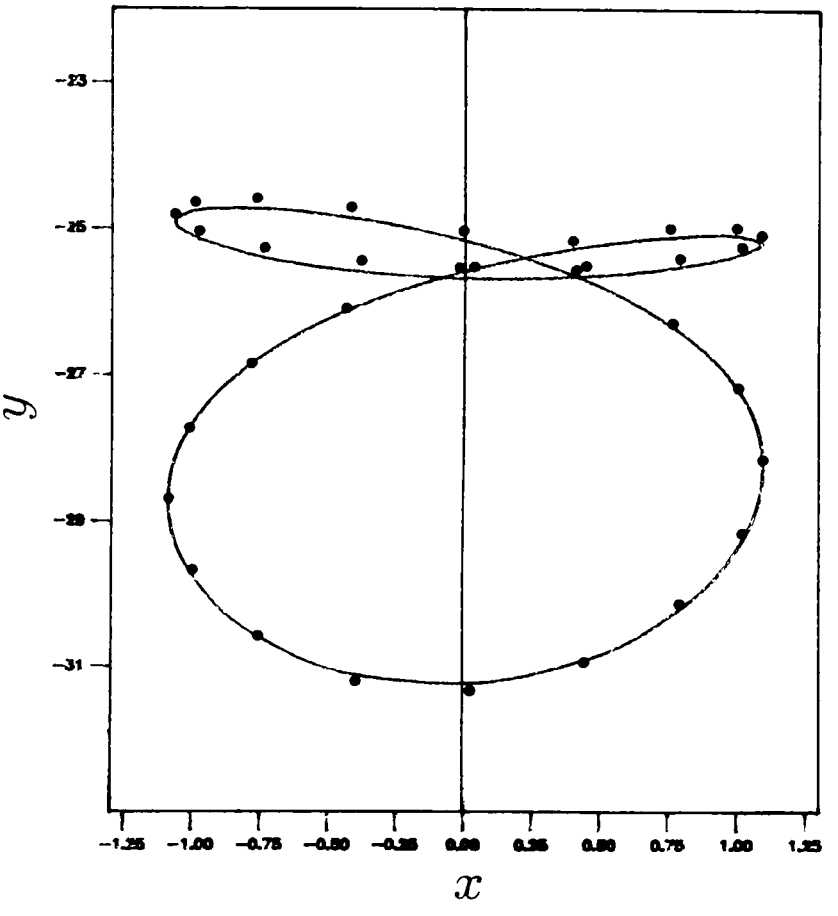

Fig. 3. Orbit-2 whirling motion ($\alpha = 25$, $\zeta = 0.02$, $\Omega = 2.2$, $\gamma = 0$, $\mu = 0$) — HBM; . . . Runge-Kutta.

initial guesses and more complicated formulations involving Jacobian calculation. However, with the HBM/AFT previously calculated results can be used to guess next initial starts for consecutive calculation. It was therefore concluded that the HBM/AFT method constitutes more effective means of obtaining bifurcation boundaries.

Bifurcation Behavior

One of the major advantages of implementing the HBM/AFT method is that it can readily lead to a procedure which yields stability and bifurcation boundaries at which qualitative changes in rotor whirling occur.

First, effects of the magnitudes of the stiffness ratio α and critical damping ζ were investigated. The results show that an increase in α causes period doubling through flip bifurcation. Boundaries between stable period-1 whirling motion and stable period-2 orbits are shown in Figure 5. In this figure, a stable period-1 orbit exists outside of each curve and period-2 orbits exist inside of each curve. This figure also reveals that higher ζ may eliminate dangerous period-2 orbits with the same frequency. This result well agree with previous results [16].

Figure 6 shows the same α and ζ influence on flip bifurcation with $\Omega = 1.6$–3.0. The figure

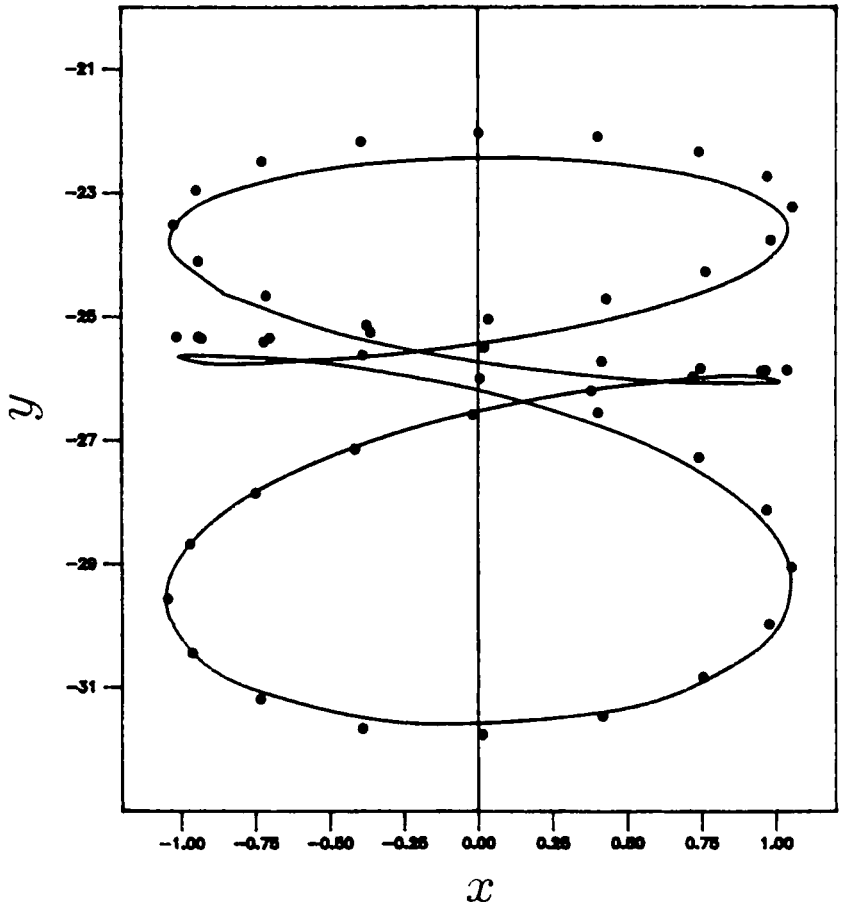

Fig. 4. Orbit-3 whirling motion ($\alpha = 25$, $\zeta = 0.02$, $\Omega = 3.2$, $\gamma = 0$, $\mu = 0$) — HBM; . . . Runge–Kutt

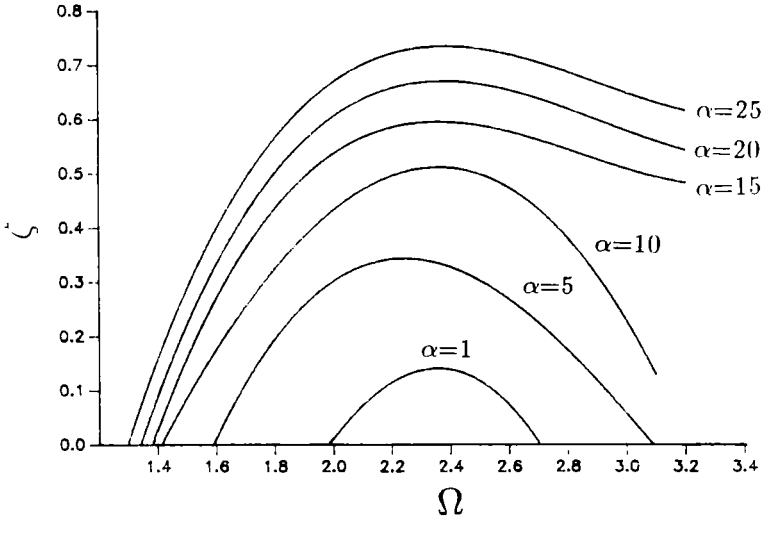

Fig. 5. First flip bifurcation boundaries in $\zeta - \Omega$ plane ($\gamma = 0$, $\mu = 0$).

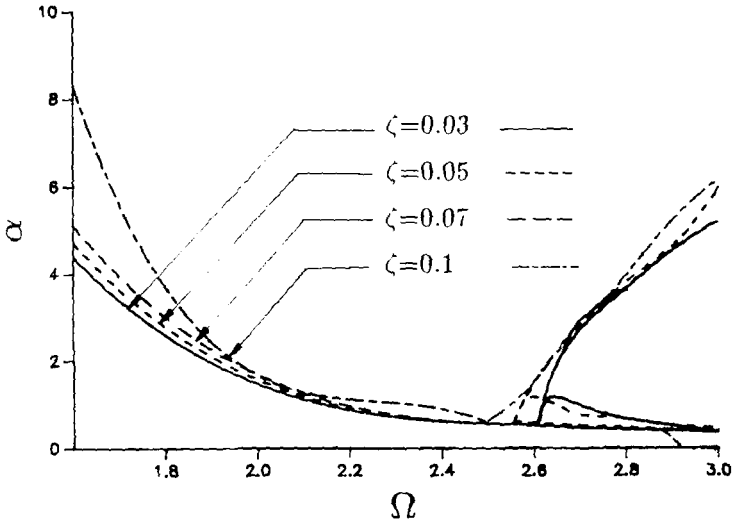

Fig. 6(a). First flip bifurcation boundaries in $\alpha - \Omega$ plane ($\Omega = 1.6$–3.0, $\gamma = 0$, $\mu = 0$).

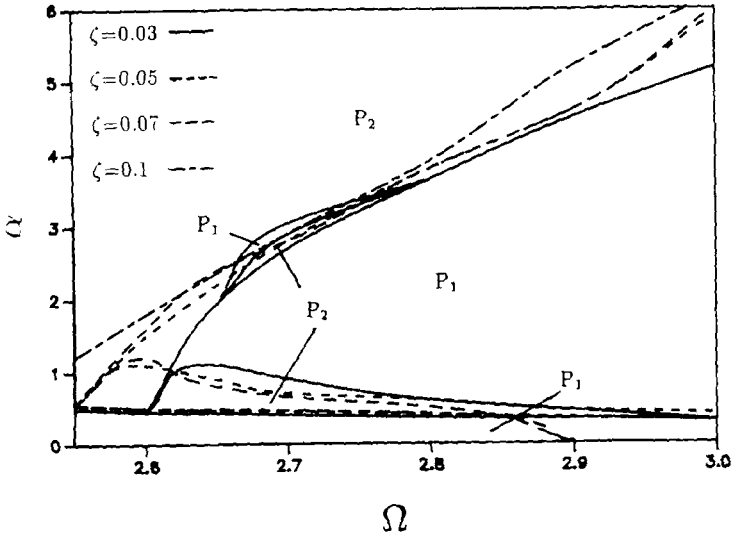

Fig. 6(b). First flip bifurcation boundaries in $\alpha - \Omega$ plane ($\Omega = 2.55$–3.0, $\gamma = 0$, $\mu = 0$); P_1 = period-1 whirling; P_2 = period-2 whirling.

reveals that there are two types of period-2 orbits possible in the range of $\Omega = 2.5$–3.0, since there are two flip boundary branches with fixed Ω. Next, the maximum magnitudes of Floquet multipliers are calculated for $\Omega = 2.7$ for different values of α and ζ as shown in Figure 7. In this figure, there are two types of period-2 orbits (denoted as type A and type B) which are possible with ζ less than 0.1. These two types of period-2 whirling motions are confirmed by numerical integration as shown in Figure 8. Type A response could be considered to be more dangerous since it has larger amplitude. Further increase of α leads to another flip bifurcation (2nd flip bifurcation) as shown in Figure 9. This figure shows a similar ζ effect as that observed in Figure 5. In this figure period-4 orbit exists outside of each curve and period-2 orbit is located inside of each curve. It is interesting to note that at the range of $\Omega = 1.8$–2.2, higher subharmonics are difficult

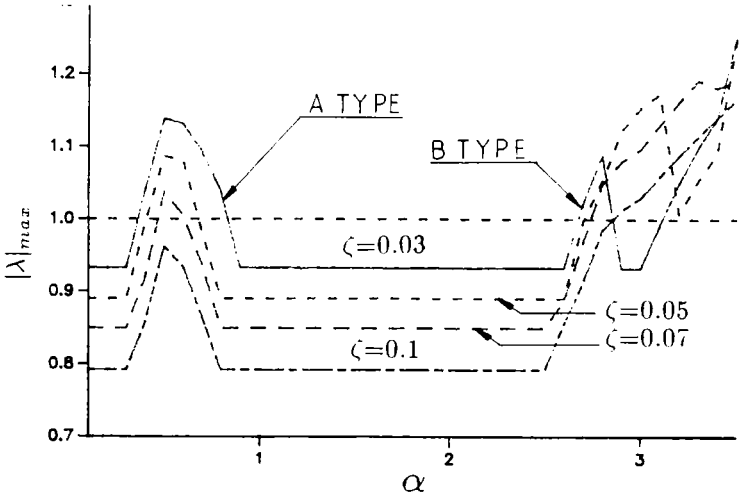

Fig. 7. Maximum magnitude of Floquet mutipliers near 1st flip bifurcation boundaries ($\Omega = 2.7$, $\gamma = 0$, $\mu = 0$).

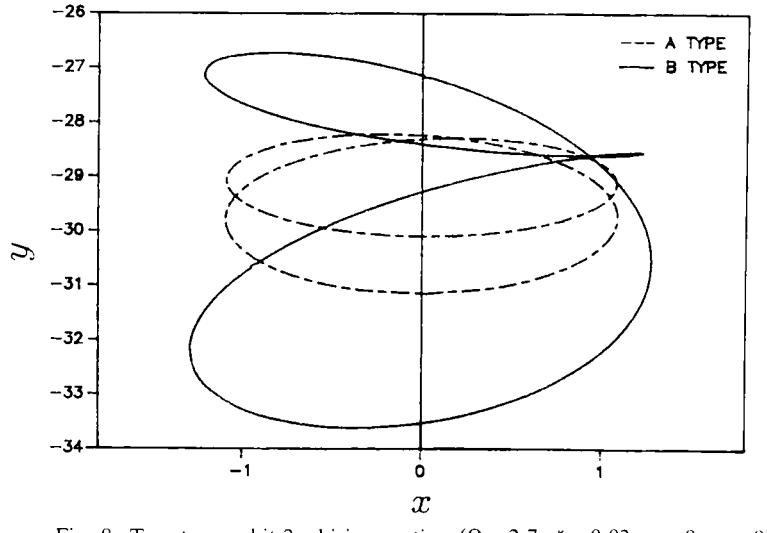

Fig. 8. Two type orbit-2 whiring motion ($\Omega = 2.7$, $\zeta = 0.03$, $\gamma = 0$, $\mu = 0$).

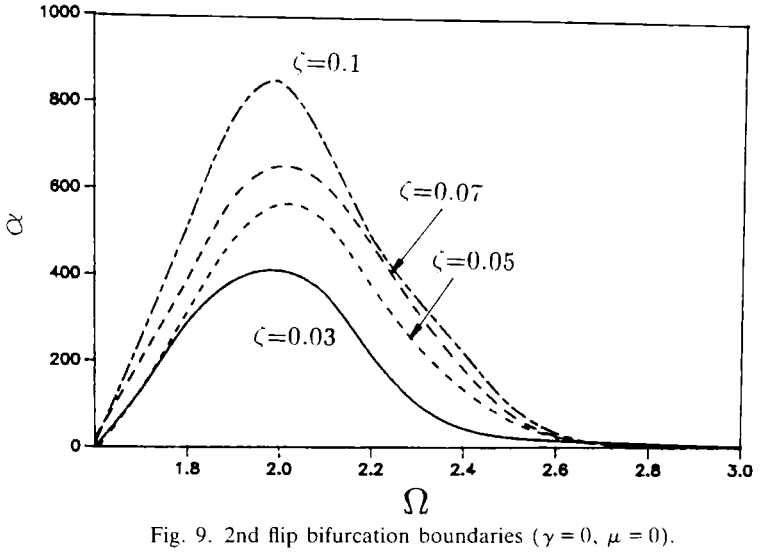

Fig. 9. 2nd flip bifurcation boundaries ($\gamma = 0$, $\mu = 0$).

to obtain unless α has very high value, which approaches an impact condition. From Figure 9 it is predicted that by increasing α, further sequences of period doubling occur leading to irregular (or chaotic) whirling motion of the nonlinear rotor system studied herein. Figures 10 (a)–(c) show this period doubling process at $\Omega = 1.6$. Figure 10 (d) shows chaotic whirling with a high α value. This chaotic motion is quite different from aperiodic whirling motion (which is discussed later). The occurrence of both types of motion is confirmed by stroboscopic snap plots at every forcing period, which is similar to the Poincaré maps in one dimensional problems.

The important characteristics of chaotic motion in the present rotor system are associated with its violent vibration which might cause severe rotor-stator interaction. Chaotic motion is also characterized by a wide-band, continuous frequency content which might lead to adverse conditions of fatigue or excitation of other coupled structures to the rotor. A remedy of this

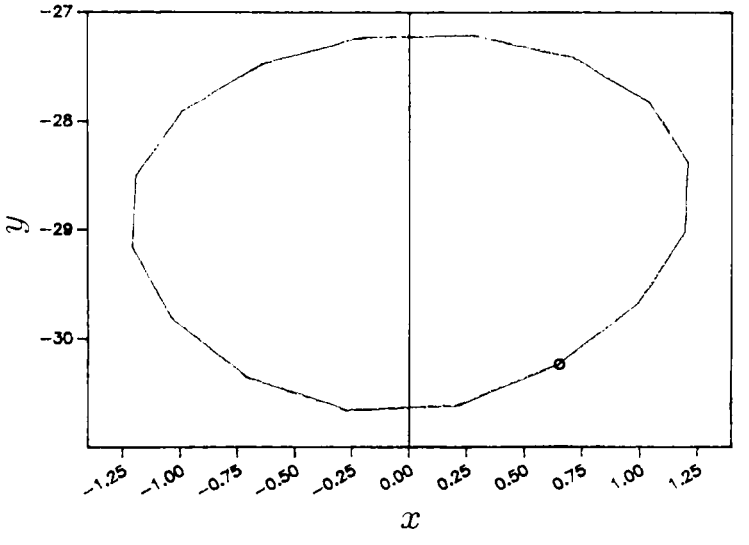

Fig. 10(a). Orbit-1 whirling motion ($\Omega = 1.6$, $\alpha = 10$, $\zeta = 0.1$, $\gamma = 0$, $\mu = 0$).

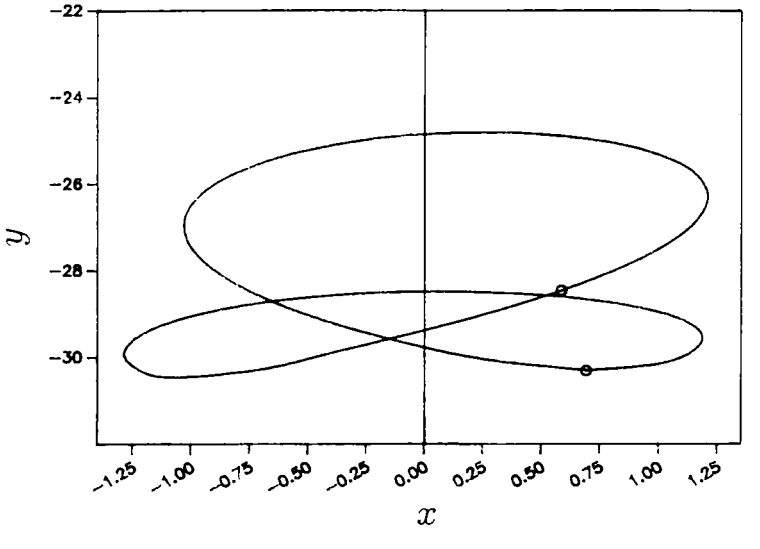

Fig. 10(b). Orbit-2 whirling motion ($\Omega = 1.6$, $\alpha = 40$, $\zeta = 0.1$, $\gamma = 0$, $\mu = 0$).

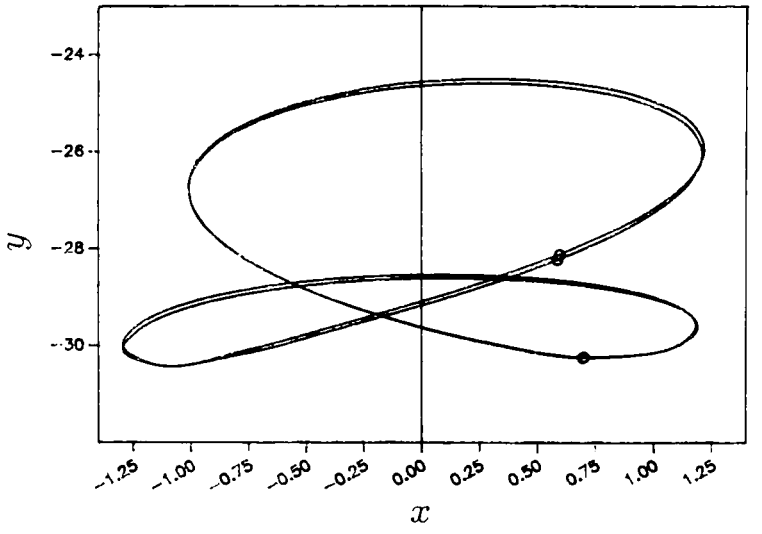

Fig. 10(c). Orbit-4 whirling motion ($\Omega = 1.6$, $\alpha = 50$, $\zeta = 0.1$, $\gamma = 0$, $\mu = 0$).

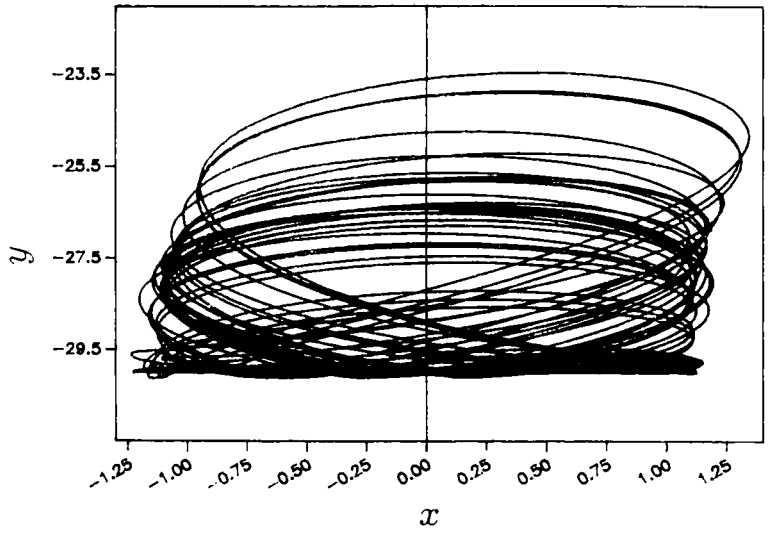

Fig. 10(d). Chaotic whirling motion ($\Omega = 1.6$, $\alpha = 100$, $\zeta = 0.1$, $\gamma = 0$, $\mu = 0$).

situation could be to increase the critical damping or to decrease the shaft-to-support stiffness ratio.

The effect of the friction coefficient, μ, between rotor and stator, is investigated and the results are shown in Figure 11 for $\Omega = 1.5$. The figure shows that higher μ tends to stabilize whirling near the flip bifurcation boundary. However, it is apparent that μ has little effect on the whirling magnitude or stability within stable orbit regions. Figure 12 shows a critical example revealing how μ affects the whirling motion near the first flip bifurcation boundary region. The figure shows that by increasing μ the period-2 orbit becomes period-1 orbit but the whirling amplitude does not change. Therefore, in critical situations, subharmonic vibration could be eliminated by increasing the magnitude of μ.

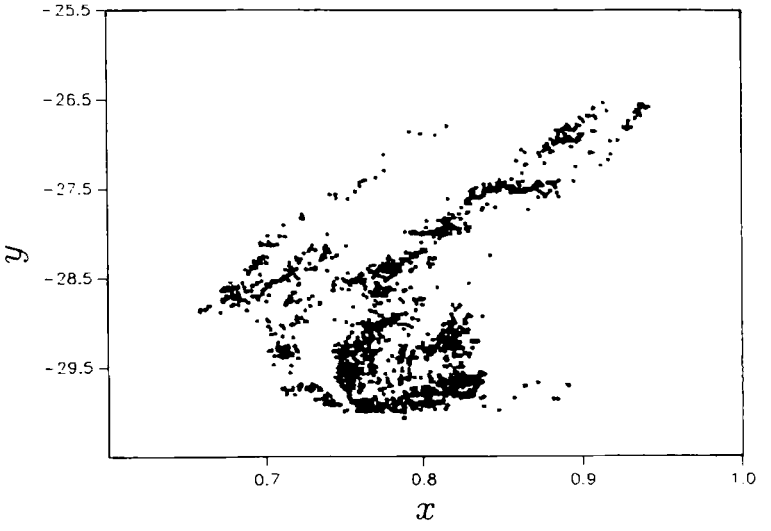

Fig. 10(e). A stroboscopic snap shot of chaotic whirling motion ($\Omega = 1.6$, $\alpha = 100$, $\zeta = 0.1$, $\gamma = 0$, $\mu = 0$).

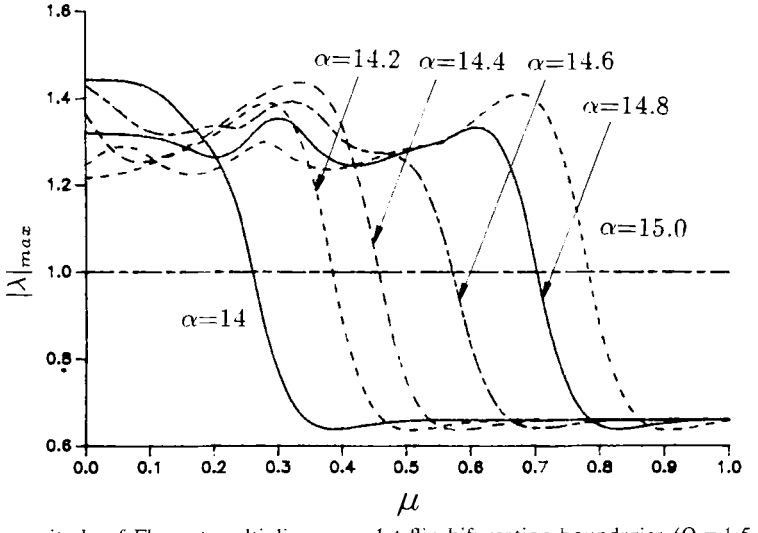

Fig. 11. Maximum magnitude of Floquet multipliers near 1st flip bifurcation boundaries ($\Omega = 1.5$, $\zeta = 0.11$, $\gamma = 0$).

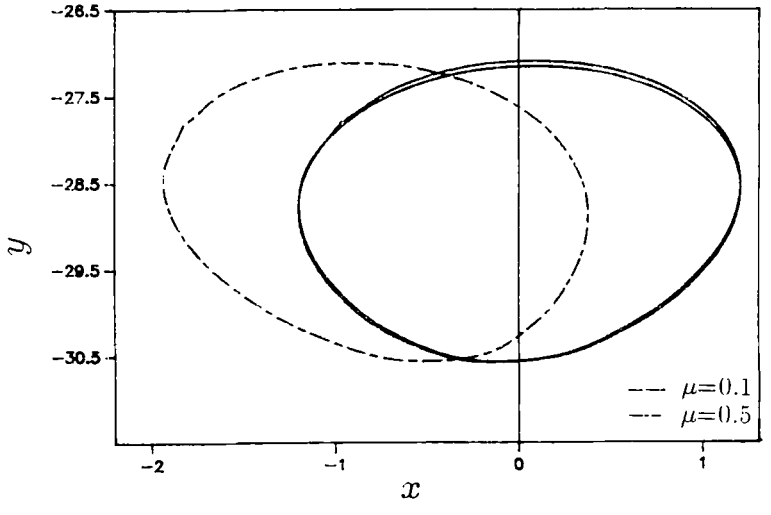

Fig. 12. Effect of μ ($\Omega = 1.5$, $\zeta = 0.11$, $\alpha = 14.4$, $\gamma = 0$) — $\mu = 0.1$; --- $\mu = 0.5$.

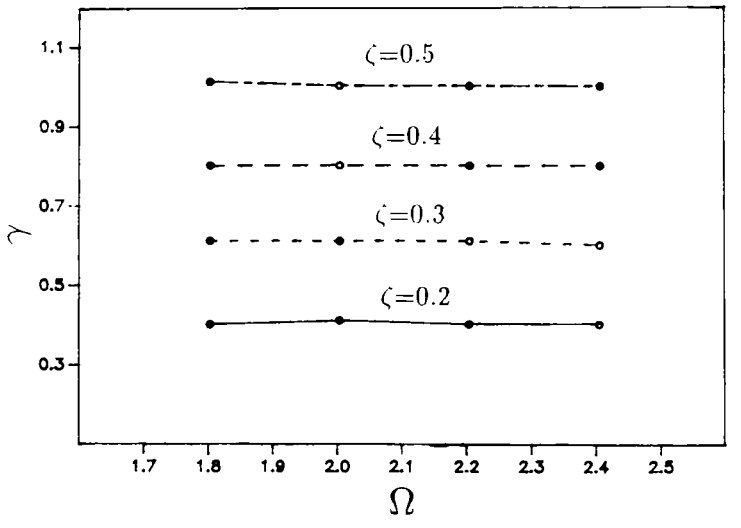

Fig. 13. Hopf bifurcation boundaries ($\alpha = 1$, $\mu = 0$).

Finally the effect of the cross coupling stiffness, γ, is investigated and the results are shown in Figure 13. It is seen that the change in γ results in a different type of bifurcation. A Hopf bifurcation can exist in this case (two complex conjugate multipliers leave the unit circle while the other two remain inside of the unit circle). In Figure 13, the period-1 orbit exists below each line and a Hopf bifurcation occurs above that line. A Hopf bifurcation produces aperiodic (or quasi-periodic) motion as shown in Figure 14. The figure shows that the aperiodic motion has two different frequency components (which are incommensurate) and much larger whirling amplitude than the period-1 orbit.

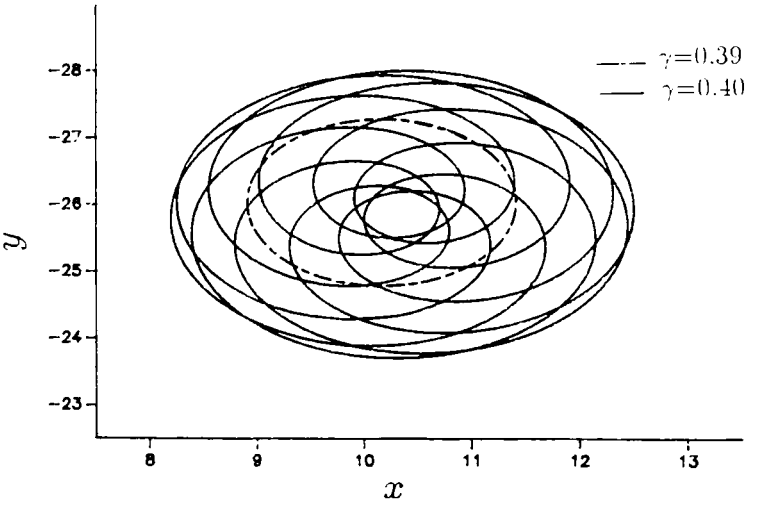

Fig. 14(a). Aperiodic whirling motion due to Hopf bifurcation ($\alpha = 1$, $\mu = 0$) --- $\gamma = 0.39$; — $\gamma = 0.40$.

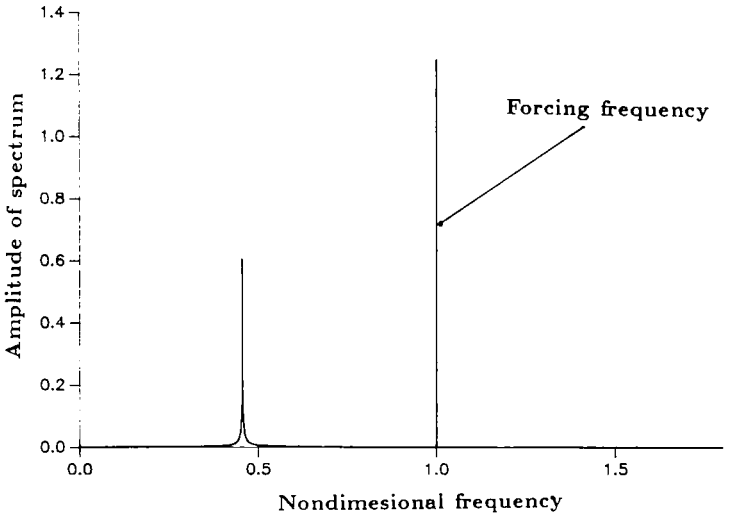

Fig. 14(b). Power spectrum of aperiodic whirling motion ($\alpha = 1$, $\mu = 0$, $\gamma = 0.40$).

Conclusion

A robust iterative numerical procedure based on the HBM/AFT method has been presented for obtaining the periodic responses of a rotor system on nonlinear supports. Modern bifurcation theory is utilized to characterize the dynamic behavior of the system. A bifurcation analysis method is developed which provides boundaries of parameter regions at which rotor whirling change its shape rapidly, resulting in the occurrence of subharmonic, aperiodic or possible chaotic motion.

The results of this study lead to the following observations concerning the dynamic behavior of the nonlinear, modified Jeffcott rotor model considered herein as function of its dimensionless parameters:

1. Increasing the bearing to shaft stiffness ratio, α, increases the degree of nonlinearity which makes it possible for a flip bifurcation to occur, possibly producing a sequence of period doubling motions.
2. For the same α and Ω, an increase in ζ leads to elimination of the subharmonic motion.
3. With high values of α, occurrence of chaotic whirling motion is possible. This follows from (1).
4. For the parameters considered herein, the coefficient of friction, μ, has little effect on the subharmonic response. However, higher μ could eliminate the subharmonics near existing flip bifurcation boundaries.
5. Increasing the cross coupling coefficient, γ, could cause a Hopf bifurcation to occur which may lead to aperiodic whirling. A more systematic investigation of the quasi-periodic response of nonlinear rotor systems is needed. A nonzero value of γ is necessary for the occurrence of aperiodic solution. This is since in this case a limit cycle can exist in absence of imbalance forces. A quasi-periodic response then occurs in presence of an imbalance force involving a frequency related to that of the limit cycle and the forcing frequency, or rotational speed of the shaft.

Acknowledgement

This work was carried out as part of a research project supported by NASA, Marshall Flight Center under contract No. NAS8-37465. The authors are grateful to Thomas Fox, the technical monitor, for his enthusiastic support and interest.

Appendix A

Elements of the Jacobian matrix, $[J]$

$$J_{4n-1,4n-1} = \frac{\partial g_{4n-1}}{\partial a_{xn}} = -n^2 + t_1 + \frac{\partial c_{xn}}{\partial a_{xn}} - \mu \frac{\partial c_{yn}}{\partial a_{xn}}$$

$$J_{4n-1,4n} = \frac{\partial g_{4n-1}}{\partial b_{xn}} = -nt_2 + \frac{\partial c_{xn}}{\partial b_{xn}} - \mu \frac{\partial c_{yn}}{\partial b_{xn}}$$

$$J_{4n-1,4n+1} = \frac{\partial g_{4n-1}}{\partial a_{yn}} = t_3 + \frac{\partial c_{xn}}{\partial a_{yn}} - \mu \frac{\partial c_{yn}}{\partial a_{yn}}$$

$$J_{4n-1,4n+2} = \frac{\partial g_{4n-1}}{\partial b_{yn}} = \frac{\partial c_{xn}}{\partial b_{yn}} - \mu \frac{\partial c_{yn}}{\partial b_{yn}}$$

$$J_{4n,4n-1} = \frac{\partial g_{4n}}{\partial a_{xn}} = -nt_2 - \frac{\partial d_{xn}}{\partial a_{xn}} + \mu \frac{\partial d_{yn}}{\partial a_{xn}}$$

$$J_{4n,4n} = \frac{\partial g_{4n}}{\partial b_{xn}} = n^2 - t_1 - \frac{\partial d_{xn}}{\partial b_{xn}} + \mu \frac{\partial d_{yn}}{\partial b_{xn}}$$

$$J_{4n,4n+1} = \frac{\partial g_{4n}}{\partial a_{yn}} = -\frac{\partial d_{xn}}{\partial a_{yn}} + \mu \frac{\partial d_{yn}}{\partial a_{yn}}$$

$$J_{4n,4n+2} = \frac{\partial g_{4n}}{\partial b_{yn}} = -t_3 - \frac{\partial d_{xn}}{\partial b_{yn}} + \mu \frac{\partial d_{yn}}{\partial b_{yn}}$$

$$J_{4n+1,4n-1} = \frac{\partial g_{4n+1}}{\partial a_{xn}} = -t_3 + \frac{\partial c_{yn}}{\partial a_{xn}} + \mu \frac{\partial c_{xn}}{\partial a_{xn}}$$

$$J_{4n+1,4n} = \frac{\partial g_{4n+1}}{\partial b_{xn}} = +\frac{\partial c_{yn}}{\partial b_{xn}} + \mu \frac{\partial c_{xn}}{\partial b_{xn}}$$

$$J_{4n+1,4n+1} = \frac{\partial g_{4n+1}}{\partial a_{yn}} = -n^2 + t_1 + \frac{\partial c_{yn}}{\partial a_{yn}} + \mu \frac{\partial c_{xn}}{\partial a_{yn}}$$

$$J_{4n+1,4n+2} = \frac{\partial g_{4n+1}}{\partial b_{yn}} = -nt_2 + \frac{\partial c_{yn}}{\partial b_{yn}} + \mu \frac{\partial c_{xn}}{\partial b_{yn}}$$

$$J_{4n+2,4n-1} = \frac{\partial g_{4n+2}}{\partial a_{xn}} = -\frac{\partial d_{yn}}{\partial a_{xn}} - \mu \frac{\partial d_{xn}}{\partial a_{xn}}$$

$$J_{4n+2,4n} = \frac{\partial g_{4n+2}}{\partial b_{xn}} = t_3 - \frac{\partial d_{yn}}{\partial b_{xn}} - \mu \frac{\partial d_{xn}}{\partial b_{xn}}$$

$$J_{4n+2,4n+1} = \frac{\partial g_{4n+2}}{\partial a_{yn}} = -nt_2 - \frac{\partial d_{yn}}{\partial a_{yn}} - \mu \frac{\partial d_{xn}}{\partial a_{yn}}$$

$$J_{4n+2,4n+2} = \frac{\partial g_{4n+2}}{\partial b_{yn}} = n^2 - t_1 - \frac{\partial d_{yn}}{\partial b_{yn}} - \mu \frac{\partial d_{xn}}{\partial b_{yn}}$$

where

$$t_1 = \frac{\nu^2}{\Omega^2} \frac{(1+\sqrt{\alpha})^2}{4\alpha}, \qquad t_2 = \frac{2\zeta\nu}{\Omega}, \qquad t_3 = \gamma \frac{\nu^2}{\Omega^2}.$$

Appendix B

Calculation of elements of $[J]$

Using

$$T(x, y) = \Phi \frac{\nu^2}{\Omega^2} \frac{(1+\sqrt{\alpha})^2}{4} x\left(1 - \frac{\delta^*}{\sqrt{x^2+y^2}}\right) \tag{B1}$$

$$F(x, y) = \Phi \frac{\nu^2}{\Omega^2} \frac{(1+\sqrt{\alpha})^2}{4} y\left(1 - \frac{\delta^*}{\sqrt{x^2+y^2}}\right) \tag{B2}$$

the incremental form is expressed as

$$\Delta T(x, y) = \left(\frac{\partial T}{\partial x}\Delta x + \frac{\partial T}{\partial y}\Delta y\right) = A\Delta x - B\Delta y \tag{B3}$$

$$\Delta F(x, y) = \left(\frac{\partial N}{\partial x}\Delta x + \frac{\partial N}{\partial y}\Delta y\right) = -C\Delta x + D\Delta y \tag{B4}$$

where

$$A = \Phi \frac{\nu^2}{\Phi^2}\left\{\frac{(1+\sqrt{\alpha})^2}{4} - \frac{(1+\sqrt{\alpha})^2}{4}\delta^*(x^2+y^2)^{-3/2}y^2\right\}$$

$$B = -\Phi \frac{\nu^2}{\Omega^2}\left\{\frac{(1+\sqrt{\alpha})^2}{4}\delta^*(x^2+y^2)^{-3/2}xy\right\}$$

$$C = -\Phi \frac{\nu^2}{\Omega^2}\left\{\frac{(1+\sqrt{\alpha})^2}{4}\delta^*(x^2+y^2)^{-3/2}xy\right\}$$

$$D = \Phi \frac{\nu^2}{\Omega^2}\left\{\frac{(1+\sqrt{\alpha})^2}{4} - \frac{(1+\sqrt{\alpha})^2}{4}\delta^*(x^2+y^2)^{-3/2}x^2\right\}.$$

Also, the Δx and Δy are

$$\Delta x = \frac{\partial x}{\partial a_{x0}}\Delta a_{x0} + \sum_{n=1}^{N}\left(\frac{\partial x}{\partial a_{xn}}\Delta a_{xn} - \frac{\partial x}{\partial b_{xn}}\Delta b_{xn}\right) = \Delta a_{x0} + \sum_{n=1}^{N}(\Delta a_{xn}\cos n\theta - \Delta b_{xn}\sin n\theta), \tag{B5}$$

$$\Delta y = \frac{\partial y}{\partial a_{x0}} \Delta a_{y0} + \sum_{n=1}^{N} \left(\frac{\partial y}{\partial a_{yn}} \Delta a_{yn} - \frac{\partial y}{\partial b_{yn}} \Delta b_{yn} \right) = \Delta a_{y0} + \sum_{n=1}^{N} (\Delta a_{yn} \cos n\theta - \Delta b_{yn} \sin n\theta) . \tag{B6}$$

Similarly, from equation (4), ΔT and ΔF can be expressed as

$$\Delta T = \Delta c_{x0} + \sum_{n=1}^{N} (\Delta c_{xn} \cos n\theta - \Delta d_{xn} \sin n\theta) , \tag{B7}$$

$$\Delta F = \Delta c_{y0} + \sum_{n=1}^{N} (\Delta c_{yn} \cos n\theta - \Delta d_{yn} \sin n\theta) , \tag{B8}$$

From equations (B3), (B4), (B7) and (B8), and using Galerkin's method, one can get the following expressions for determining the elements of $[J]$. (The utilization of Galerkin's method rather than DFT and IDFT makes it much easier to obtain the $\partial \mathbf{Q}/\partial \mathbf{P}$ for the present two dimensional system.)

$$\begin{aligned}
&\int_0^T A\left\{\Delta a_{x0} + \sum_{n=1}^{N} (\Delta a_{xn} \cos n\theta - \Delta b_{xn} \sin n\theta)\right\}\{\cos\theta, \ldots, \sin\theta\}^T \, d\theta \\
&- \int_0^T B\left\{\Delta a_{y0} + \sum_{n=1}^{N} (\Delta a_{yn} \cos n\theta - \Delta b_{yn} \sin n\theta)\right\}\{\cos\theta, \ldots, \sin n\theta\}^T \, d\theta = \\
&\int_0^T A\left\{\Delta c_{x0} + \sum_{n=1}^{N} (\Delta c_{xn} \cos n\theta - \Delta d_{xn} \sin n\theta)\right\}\{\cos\theta, \ldots, \sin n\theta\}^T \, d\theta ,
\end{aligned} \tag{B9}$$

$$\begin{aligned}
&- \int_0^T C\left\{\Delta a_{x0} + \sum_{n=1}^{N} (\Delta a_{xn} \cos n\theta - \Delta b_{xn} \sin n\theta)\right\}\{\cos\theta, \ldots, \sin n\theta\}^T \, d\theta \\
&+ \int_0^T D\left\{\Delta a_{y0} + \sum_{n=1}^{N} (\Delta a_{yn} \cos n\theta - \Delta b_{yn} \sin n\theta)\right\}\{\cos\theta, \ldots, \sin n\theta\}^T \, d\theta = \\
&\int_0^T A\left\{\Delta c_{y0} + \sum_{n=1}^{N} (\Delta c_{yn} \cos n\theta - \Delta d_{yn} \sin n\theta)\right\}\{\cos\theta, \ldots, \sin n\theta\}^T \, d\theta ,
\end{aligned} \tag{B10}$$

where the upper limit of integration, T, is 2π. Using equations (B9), (B10), the first derivatives, $\partial \mathbf{Q}/\partial \mathbf{P}$, for the Jacobian matrix are obtained as listed in equations (13) in text.

References

1. Bently, D., 'Forced subrotative speed dynamic action of rotating machinery', *ASME* paper No. 74-PET-16; *Petroleum Mechanical Engineering Conference*, Dallas, Texas, 1974.
2. Childs, D. W., 'Fractional-frequency rotor motion due to nonsymmetric clearance effects', *ASME Journal of Energy and Power* **104**, 1982, 533–541.
3. Saito, S., 'Calculation of nonlinear unbalance response of horizontal Jeffcott rotors supported by ball bearings with radial clearances', *ASME paper No. 85-DET-33*, 1985.
4. Yamauchi, S., 'The nonlinear vibration of flexible rotors, 1st report, Development of a new analysis technique', *JSME* **49**, No. 446, Series C, 1983, 1862–1868.
5. Choi, Y. S. and S. T. Noah, 'Nonlinear steady-state response of a rotor-support system', *ASME Journal of Vibration, Acoustics, Stress, and Reliability in Design* **109**, 1987, 255–261.

6. Nataraj, C. and H. D. Nelson, 'Periodic solutions in rotor dynamic systems with nonlinear supports: A general approach', *ASME Design Conference*, Oct. 1987.
7. Ehrich, F. F., High order subharmonic response of high speed rotors in bearing clearance', *ASME Journal of Vibration, Acoustics, Stress, and Reliability in Design* **110**, 1988, 9–16.
8. Childs, D. W., 'Rotordynamic characteristics of the HPOTP (High Pressure Oxygen Turbopump) of the SSME (Space Shuttle Main Engine)', Turbomachinery Laboratories Report (Texas A&M Univ.) FD-1-84, 1984.
9. Day, W.B., 'Asymptotic expansions in nonlinear rotordynamics', *Quarterly of Applied Mathematics* **44**, 1987, 779–792.
10. Shaw, S. W. and J. P. Holmes, 'A periodically forced piecewise-linear oscillator', *Journal of Sound and Vibration* **108**, 1983, 129–155.
11. Natsiavas, S., 'Periodic response and stability of oscillators with symmetric trilinear restoring force', *Journal of Sound and Vibration* **134**, 1989, 315–331.
12. Dennis, Jr., J. E., and J. J. More, 'Quasi-Newton method, motivation and theory', *SIAM Review* **19**, 1977, 46–88.
13. Kim, Y. B. and Noah, S. T., 'Stability and bifurcation analysis of oscillators with piecewise-smooth characteristics: A general approach', accepted for publication in ASME *J. of Applied Mechanics*, 1990.
14. Hale, J. K., *Oscillators in Nonlinear Systems*, McGraw-Hill, New York, 1963.
15. Guckenheimer J and J. P. Holmes, *Nonlinear Oscillations, Dynamical Systems, and Bifurcation of Vector Fields*, Springer-Verlag, 1983.
16. Kim, Y. B. and Noah, S. T., 'Steady-state analysis of a nonlinear rotor-housing system', to appear in ASME *Journal of Turbomachinery*, 1989. Also ASME paper No. 90-GT-328.